Journal of Power Sources 189 (2009) 794–797

Contents lists available at ScienceDirect

Journal of Power Sources

journal homepage: www.elsevier.com/locate/jpowsour

Short communication

Preparation and characterization of mesoporous $LiFePO_4$/C microsphere by spray drying assisted template method

Feng Yu[a,b], Jingjie Zhang[a,*], Yanfeng Yang[a], Guangzhi Song[a]

[a] Technical Institute of Physics and Chemistry, Chinese Academy of Sciences, Beijing 100190, China
[b] Graduate University of Chinese Academy of Sciences, Beijing 100049, China

ARTICLE INFO

Article history:
Received 15 May 2008
Received in revised form 22 July 2008
Accepted 24 July 2008
Available online 3 August 2008

Keywords:
$LiFePO_4$/C
Mesoporous microsphere
Spray drying
Template

ABSTRACT

Mesoporous $LiFePO_4$/C microsphere was successfully prepared by spray drying assisted template method (SDATM) with citric acid as a template. This material has an average pore size of 50 nm and gives large specific surface area (32.2 $m^2\,g^{-1}$) with evenly distributed carbon (4.3 wt.%). It is also easy to bring into contact with electrolyte, facilitate the electric and lithium ion diffusion. It presents large reversible capacity of 158.8 mAh g^{-1} at *C*/10, even high rate capacity of 59.7 mAh g^{-1} at 20*C*, and excellent capacity retention rate closed to 95.5% after various current densities.

© 2008 Published by Elsevier B.V.

1. Introduction

Rechargeable lithium-ion batteries have a higher energy density than conventional lead–acid, nickel–cadmium, and even nickel–metal hydride batteries. They are the most promising candidates, which are needed urgently to be used for application such as electric vehicles (EV) and hybrid electric vehicles (HEV), to meet demands of modern technology, and to revolutionize consumer electronics. However, the commercial layered $LiCoO_2$ material utilized as the positive electrode, suffers from high cost, toxicity, and inferior safety concerning that necessitate careful electronic control of the cell [1–3].

The lithium transition metal phosphates $LiFePO_4$ has attracted extensive interest among researchers, because these polyanionic compounds show numerous appealing features such as high theoretical capacity, acceptable operating voltage, superior safety, environmental benignity, low cost and other important advantages [2,4]. However, the poor electronic conductivity and lithium ion diffusion pose a bottleneck for the commercial applications of olivine type $LiFePO_4$ as a promising cathode material [4–6]. In a number of papers, the improvement of purity, optimization of particles, control of morphology, doping the foreign atoms and adding conductive agent have been described and studied in order to increase its conductivity and rate capability properties, but its electrochemical performance enhancement is still limited [5–11]. Recently, the porous $LiFePO_4$ material has been attracted various researchers because of a high electronic conductivity and quick Li^+ permeation [12–15].

In this paper, we present a novel and facile approach to obtain homogeneous mesoporous $LiFePO_4$/C microsphere by spray drying assisted template method (SDATM). We have realized that the homogeneous mesopores would be produced by using citric acid as a template. This material is easy to contact with electrolyte and give good electrochemical characteristics because of its large surface area and evenly carbon coated. The cycling performance of the prepared $LiFePO_4$/C cathode powders were examined with capacity retention studies performed with various *C* rates in the voltage of 2.0–4.2 V.

2. Experimental

The homogeneous mesoporous $LiFePO_4$/C microsphere had been successfully prepared by heat-treating the precursor, which was synthesized by using citric acid (small molecular organic acid) as template and spray drying. Amounts of Li_2CO_3(AR), $Fe(NO_3)_3{\cdot}9H_2O$(AR), $NH_4H_2PO_4$(AR) and citric acid were dissolved in distilled water in the stoichiometric ratio: $n_{Li}:n_{Fe}:n_P:n_{acid} = 1:1:1:x$ ($x = 0.25, 0.50, 0.75, 1.0$). The solution was sprayed in a heat reactor at 200 °C using air as the carrier gas. Then, the obtained precursor was burned out at 120 °C for 5 h in an air-limited box furnace. Finally, the obtained powders were calcined

---

[*] Corresponding author. Tel.: +86 10 82543691; fax: +86 10 82543691.
E-mail addresses: yufeng05@mail.ipc.ac.cn (F. Yu), jjzhang@mail.ipc.ac.cn (J. Zhang).

0378-7753/$ – see front matter © 2008 Published by Elsevier B.V.
doi:10.1016/j.jpowsour.2008.07.074

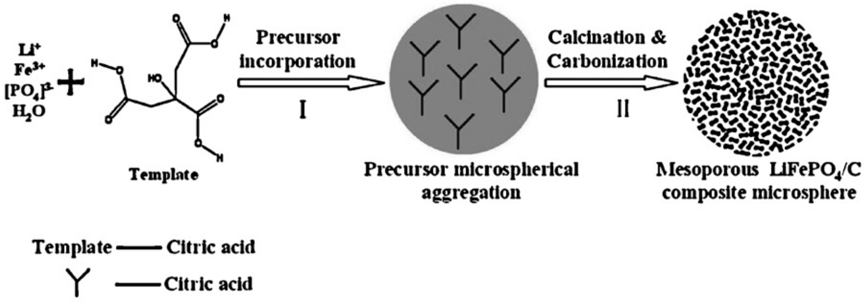

Fig. 1. Schematic illustration of mesoporous $LiFePO_4/C$ composite microsphere formation.

at 700 °C for 12 h under flowing Ar atmosphere. And the samples were signed LFPa, LFPb, LFPc and LFPd, respectively.

The crystalline structure of the prepared $LiFePO_4/C$ powders were studied by a X-ray diffractometer (*D*/max 2200 PC), with Cu Kα radiation at 40 kV, 40 mA, step size of 0.02°, and a count time of 0.6 s per step between $2\theta = 10°$ and 80°. SEM (S-4300) were used to analyze the morphology of the prepared powders. A gas sorption technique to evaluate the specific surface area by BET (NOVA4000). The carbon content of sample was determined by a carbon–sulfur analyzer (Min EA2000). Electrochemical tests were performed using CR2032 type coin cells with Lithium anode assembled in an Ar filled glove box. The electrolyte was 1.0 mol L^{-1} $LiPF_6$ in EC + DEC + DMC (1:1:1 vol.%). The cells were examined with capacity retention studies performed with various rates between 2.0 and 4.2 V. Meanwhile, the cells were retained ten minutes at 4.2 V in charging.

3. Results and discussion

To understand the formation mechanism of mesoporous $LiFePO_4/C$ microsphere, a schematic illustration is proposed in Fig. 1. It mainly consists of two steps. At the first step, the precursor microspherical aggregation is formed by spray drying with citric acid as a template, because citric acid can be evenly distributed in the form of complex compound $C_6H_5O_7Fe{\cdot}5H_2O$ in precursor solution and then uniformly distributed in the precursor microspherical aggregation. Second, homogeneous pores are formed from citrate degradation and carbonization when the precursor is heat treated. In the latter process, the carbon from the citrate acid also provides the special environment favorable for the reduction of Fe(III) and the formation of the nanocrystalline composite $LiFePO_4/C$ material.

A series of experiments were performed to explore the formation mechanism of mesoporous $LiFePO_4/C$ microsphere. Fig. 2 shows the SEM images of various $LiFePO_4/C$ samples with different citric acid addition. It can be seen that all the samples are porous microspherical with homogeneous pore sizes. The carbon is evenly distributed in the particles. It is noted that citric acid as template (in the form of complex compound $C_6H_5O_7Fe{\cdot}5H_2O$) can be uniformly distributed in the precursor by spay drying to avoid the component segregation. Then the homogeneous pores are formed due to citrate degradation when the precursor is heat treated. It is also found that the value of pore decreases from micrometer to nanometer, while the citric acid in the precursor increases from $x = 0.25$ to 1.0. Meanwhile, the carbon content and specific surface area of the $LiFePO_4/C$ samples also increase, which is shown in Table 1. When $x = 1.0$, we get the uniformly mesoporous $LiFePO_4/C$ microsphere (LFPd), which average pore diameter is about 50 nm. Obviously, this structure gives relatively larger surface area (32.2 $m^2\,g^{-1}$). It is easy to bring into contact with electrolyte, facilitate the lithium ion diffusion and lead to the reduction of the cell resistance. Moreover, the

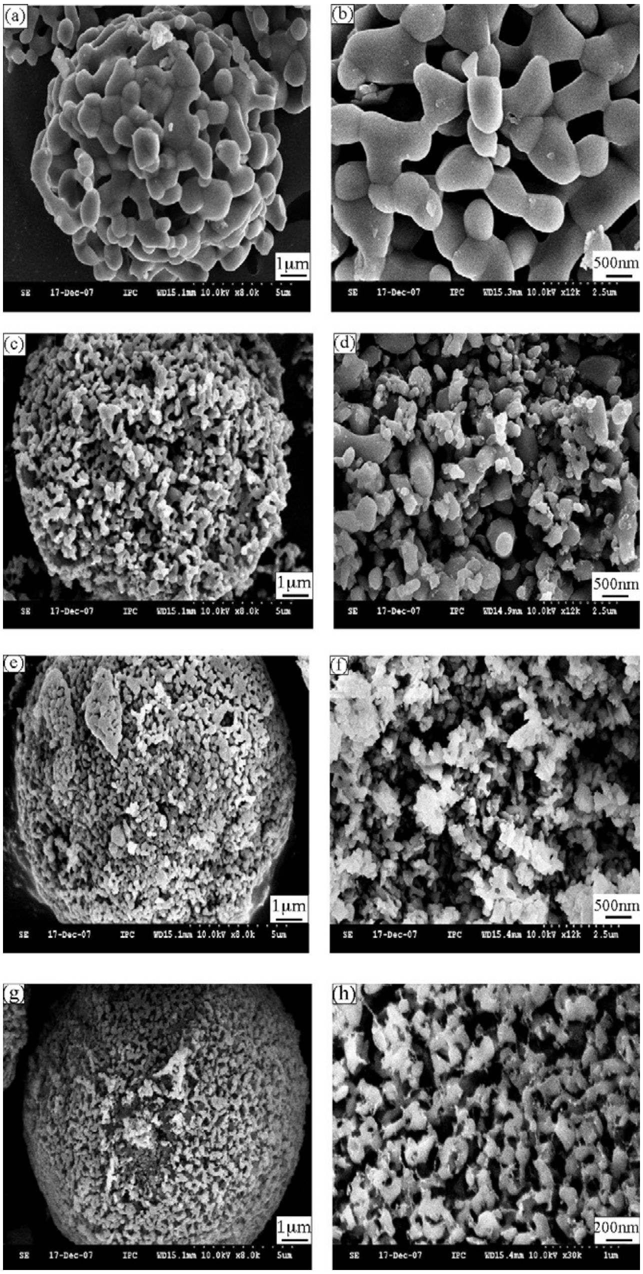

Fig. 2. SEM images of various $LiFePO_4/C$ samples. (a and b) LFPa, $x = 0.25$; (c and d) LFPb, $x = 0.50$; (e and f) LFPc, $x = 0.75$; (g and h) LFPd, $x = 1.0$.

Table 1
Carbon contents, specific surface area, calculated grain size and columbic efficiency of the first cycle for various $LiFePO_4$/C samples as a function of the nominal carbon addition

Sample	Nominal citric acid addition/*x* mol	Carbon content (wt.%)	Specific surface area ($m^2\ g^{-1}$)	Calculated grain size (nm)	Columbic efficiency of the first cycle (%)
LFPa	0.25	0.56	0.97	81–128	86.1
LFPb	0.50	0.99	7.57	68–97	88.2
LFPc	0.75	2.3	15.03	45–72	91.0
LFPd	1.0	4.3	32.25	34–52	94.7

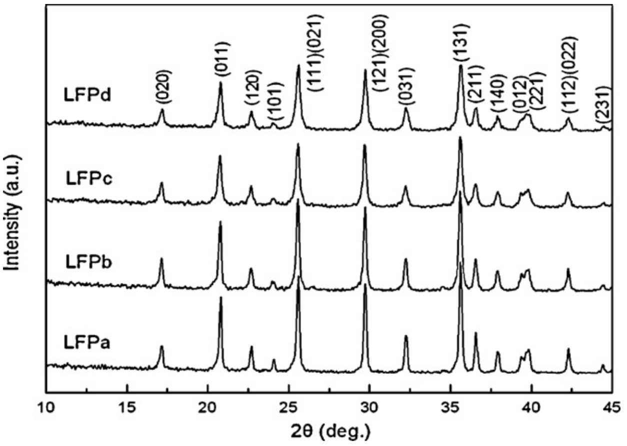

Fig. 3. X-ray diffraction patterns of various $LiFePO_4$/C samples prepared at 700 °C for 12 h.

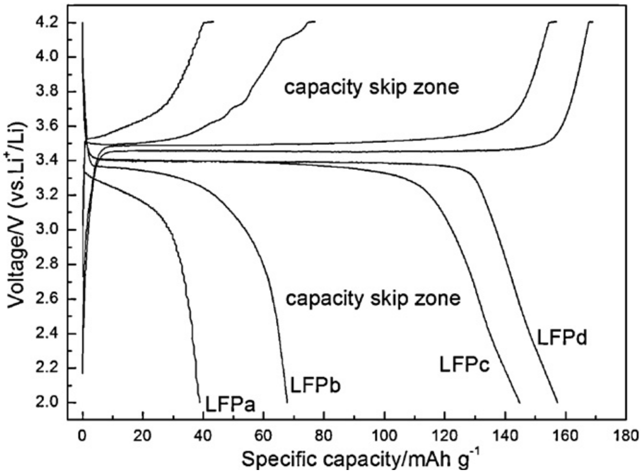

Fig. 4. Initial charge and discharge profiles of various $LiFePO_4$/C samples at room temperature cycled in the voltage of 2.0–4.2 V at *C*/10 rate (0.05 mA cm^{-2}).

evenly distributed carbon (4.3 wt.%) in the particles will enhance the electronic conductivity of the cathode materials and prevent particle coalescence. Otherwise, the $LiFePO_4$/C microsphere has excellent manufacturing performance.

The X-ray diffraction patterns of various $LiFePO_4$/C samples are shown in Fig. 3. The profiles of the reflection peaks are quite narrow and symmetric. The diffraction lines can be attributed to the monoclinic phase $LiFePO_4$ without any impurity phase. They are all in good agreement with pattern of the monoclinic $LiFePO_4$ (PDF#47-1499). Otherwise, the carbon is not detected because the residual carbon is amorphous. The absolute lattice parameters of the samples were listed in Table 2, which are close to the corresponding of PDF value and similar to the previous reports. Otherwise, it is can be seen that the half peak breadth is getting wider as the citric acid increases. This result indicates that the perfect olivine phase $LiFePO_4$ could be prepared when $x = 1.0$, and its calculated grain size is 34–52 nm much better than other samples (Table 1). The grain size results were calculated with Debye–Scherrer equation and had summarized five crystal lattice indexes of (0 1 1), (1 1 1), (1 2 1), (0 3 1) and (1 3 1).

Fig. 4 shows Initial charge and discharge profiles of various $LiFePO_4$/C samples at room temperature cycled in the voltage of 2.0–4.2 V at *C*/10 rate (0.05 mA cm^{-2}). It can be seen that the voltage profile rises rapidly from about 3.35 to 3.4 V and the specific discharge capacity increases from 37.3 mAh g^{-1} (LFPa) to 158.8 mAh g^{-1} (LFPd) at *C*/10 rate with increasing citric acid. Meanwhile, the sample LFPd electrodes deliver the charge capacity of 167.6 mAh g^{-1}, and calculation shows that the columbic efficiency during the first cycle of LFPd is about 94.7%, which is higher than that of 86.1% for LFPa (Table 1). It is also found that there is a distinct capacity skip phenomenon between $x = 0.50$ (LFPb) and $x = 0.75$ (LFPc), which may be due to the qualitative change of $LiFePO_4$/C crystallite size, carbon content and specific surface area. So we concluded that there would be lower electrode polarization and higher reversible capacity at an absolute rate when $x > 0.75$.

Cycle stabilities of various $LiFePO_4$/C samples with various discharge current rates are presented in Fig. 5. At higher rates, the superior behavior of the mesoporous $LiFePO_4$/C microsphere (LFPd) is revealed. Special reversible capacities of 112.5 and 87.2 mAh g^{-1}

Table 2
Comparison of lattice parameters of various $LiFePO_4$/C samples

Samples	*a* axis (Å)	*b* axis (Å)	*c* axis (Å)
LFPa	6.0045	10.3249	4.6864
LFPb	6.0042	10.3273	4.6879
LFPc	6.0041	10.3263	4.6883
LFPd	6.0024	10.3259	4.6853
Padhi et al. [2]	6.0083	10.3344	4.6931
Barker et al. [11]	5.971	10.288	4.676
PDF#47-1499	6.0189	10.3470	4.7039

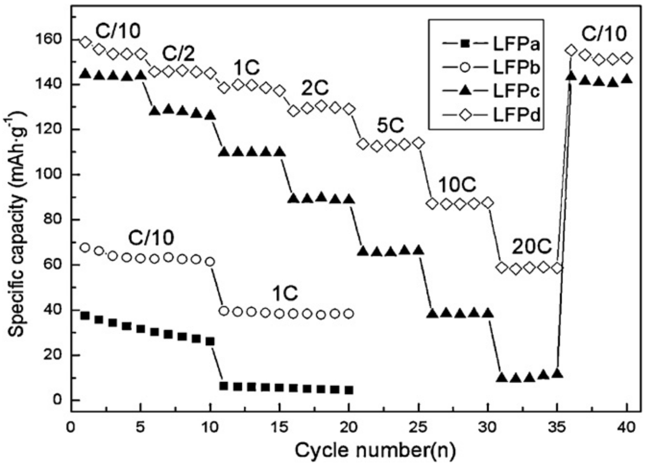

Fig. 5. Cycle stability of various $LiFePO_4$/C samples with various discharge current rates.

were obtained at rates of 5*C* and 10*C*, respectively. Even at a rate as high as 20*C*, a reversible capacity of 59.7 mAh g^{-1} can be achieved, which confirm rate capabilities with 37.6% of the maximum capacity (158.8 mAh g^{-1} at *C*/10), whereas the value drops to 9.4 mAh g^{-1} for the sample LFPc. On the other hand, when the lower current density was applied, the electrode was able to retrieve its capacity, which confirms nearly 95.5% of the starting discharge capability. This retention of $LiFePO_4$/C on extended cycling shows that the $LiFePO_4$/C possesses an excellent rate capability and good cycle life. It could be attributed to the morphology of mesoporous microsphere and highly uniform distribution of carbon in the $LiFePO_4$ particles. The $LiFePO_4$/C sample with this special morphology has perfect olivine phase, smaller particle size, and more specific surface area, which can easily bring into contact with electrolyte and facilitate the lithium ion diffusion. Meanwhile, the uniform distribution of carbon can easily enhance the electronic conductivity. The small observed voltage polarization also suggests that the $LiFePO_4$/C electrode have high electrochemical reversibility. It exhibits good reversible capacity and a capacity retention rate. It is noted that mesoporous $LiFePO_4$/C composite microsphere material has the adequate electronic conductivity, good cyclic capacity and electrochemical stability.

4. Conclusions

The homogeneous mesoporous $LiFePO_4$/C composite microsphere have been successfully prepared by spray drying assisted template method (SDATM). The value of pore and crystallite size both decreases from micrometer to nanometer with increasing carbon content and specific surface area of $LiFePO_4$/C, when the citric acid in the precursor increases from $x = 0.25$ to 1.0. When $x = 1.0$, the sample is easiest to contact with electrolyte and give best electrochemical characteristics, such as largest reversible capacity of 158.8 mAh g^{-1} at *C*/10, best rate capability of 59.7 mAh g^{-1} at 20*C*, and excellent cyclic stability which retrieve nearly 95.5% of the starting capability in 40th cycles after discharging at various rates.

References

[1] B. Scrosati, Nature 373 (1995) 557–558.
[2] A.K. Padhi, K.S. Nanjundaswamy, J.B. Goodenough, J. Electrochem. Soc. 144 (1997) 1188–1194.
[3] M.S. Whittingham, Chem. Rev. 104 (2004) 4271–4301.
[4] R. Dominko, M. Bele, M. Gaberscek, M. Remskar, D. Hanzel, J.M. Goupil, et al., J. Power Sources 153 (2006) 274–280.
[5] H.M. Xie, R.S. Wang, J.R. Ying, L.Y. Zhang, A.F. Jalbout, H.Y. Yu, et al., Adv. Mater. 18 (2006) 2609–2613.
[6] D.K. Kim, H.M. Park, S.J. Jung, Y.U. Jeong, J.H. Lee, J.J. Kim, J. Power Sources 159 (2006) 237–240.
[7] S.L. Bewlay, K. Konstantinov, G.X. Wang, S.X. Dou, H.K. Liu, Mater. Lett. 58 (2004) 1788–1791.
[8] S.H. Wu, K.M. Hsiao, W.R. Liu, J. Power Sources 146 (2005) 550–554.
[9] C. Alvaro, C.Y. Manuel, M. Julian, S.P. Jesus, R.C. Enrique, Eur. J. Inorg. Chem. 2006 (2006) 1758–1764.
[10] G.X. Wang, S.L. Bewlay, K. Konstantinov, H.K. Liu, S.X. Dou, J.H. Ahn, Electrochem. Acta 50 (2004) 443–447.
[11] J. Barker, M.Y. Saidi, J.L. Swoyer, Electrochem. Solid State Lett. 6 (2003) A53–A55.
[12] Y.S. Hu, Y.G. Guo, R. Dominko, M. Gaberscek, J. Jamnik, J. Mater. Adv. Mater. 19 (2007) 1963–1966.
[13] M. Gaberscek, R. Dominko, M. Bele, M. Remskar, D. Hanzel, J. Jamnik, Solid State Ionics 176 (2005) 1801–1805.
[14] F. Yu, J.J. Zhang, Y.F. Yang, S.L. Pan, Z.G. An, G.Z. Song, J. Funct. Mater. 38 (A04) (2007) 1390–1393.
[15] R. Dominko, M. Bele, J.M. Goupil, M. Gaberscek, D. Hanzel, I. Arcon, Chem. Mater. 19 (2007) 2960–2969.